PHYSICAL REVIEW C VOLUME 1, NUMBER 1 JANUARY 1970

# Activation Cross Sections for $(n, 2n)$ Reactions at 14.4 MeV in the Region $Z = 40$–60: Precision Measurements and Systematics*

Wen-deh Lu,† N. RanaKumar,‡ and R. W. Fink

*School of Chemistry, Georgia Institute of Technology, Atlanta, Georgia 30332*

(Received 11 August 1969)

Activation cross sections for the $(n, 2n)$ reaction in the region of $Z=40$–60 at $14.4\pm0.3$ MeV have been measured by using the mixed-powder method and Ge(Li) $\gamma$-ray detection. The total cross sections $(m+g)$ measured are (in mb) $Zr^{90}$, $652\pm31$; $Zr^{96}$, $1456\pm80$; $Mo^{92}$, $217\pm18$; $Mo^{100}$, $1389\pm84$; $Ru^{96}$, $569\pm30$; $Ru^{98}$, $1168\pm96$; $Ru^{104}$, $1440\pm80$; $Rh^{103}$, $957\pm57$; $Pd^{102}$, $637\pm45$; $Pd^{110}$, $1416\pm150$; $Cd^{108}$, $865\pm100$; $Cd^{110}$, $1221\pm150$; $Cd^{116}$, $1389\pm71$; $Sn^{114}$, $1239\pm130$; $Sb^{121}$, $1615\pm63$; $Sb^{123}$, $1542\pm80$; $Te^{122}$, $1615\pm110$; $Te^{128}$, $1661\pm161$; $Te^{130}$, $1455\pm55$; $I^{127}$, $1649\pm80$; $Cs^{133}$, $1542\pm75$; $Ba^{132}$, $1574\pm100$; $Ce^{136}$, $1318\pm90$; $Ce^{140}$, $1593\pm130$; and $Ce^{141}$, $1730\pm170$. Some partial $(n, 2n)$ cross sections also are reported. The measured values are compared with the semiempirical predictions of Pearlstein and of Gardner. No significant shell effects are seen, and the data suggest that 14-MeV $(n, 2n)$ reactions are governed predominantly by the statistical model of the compound nucleus. An empirical fit for the ratio of neutron emission to all modes of compound-nucleus decay, $\sigma_{n,M}/\sigma_{ne}$, is deduced from the present results.

## I. INTRODUCTION

By using the statistical model approach, attempts[1–3] have been made to interpret measured $(n, 2n)$ cross sections semiempirically. Pearlstein[2] calculated $(n, 2n)$ cross sections (14–15 MeV) for individual nuclides from the statistical model, together with an empirical formula to account for competition from other reactions. Gardner[3] calculated the ratios of the $(n, 2n)$ reaction cross sections of adjacent isotopes of the elements. These ratios were then semiempirically normalized to predict absolute $(n, 2n)$ cross sections. The predictions from both sets of calculations agree equally well with the relatively poor experimental data then available. Although the two methods give significantly different predictions in a number of cases, they could not be distinguished owing to gross disagreements in the existing experimental cross sections. No attempt has been made so far to compare both sets of predictions with accurate experimental values.

The existing experimental values were obtained by various workers using different experimental methods and somewhat different neutron energies between 14 and 15 MeV, and the data have relatively large errors and gross disagreements. In addition, the earlier data appear to contain some hidden systematic errors, as reflected in the gross disagreements for the same reaction. Notwithstanding the poor data, however, "shell effects" were observed in the $(n, 2n)$ cross sections.[4–6] On the other hand, later investigators[7–9] reported that shell-structure effects are relatively minor or absent.

In the present study, therefore, the $(n, 2n)$ cross sections for elements with $Z=40$–60 were measured accurately at 14.4 MeV by the activation method using Ge(Li) detection and mixed monitor and sample powders.[10] The $Z=40$–60 region was selected because in this region there are a number of isotopes of each element whose $(n, 2n)$ products are radioactive and offer good possibilities for accurate measurement by means of $\gamma$ detection. The $(n, 2n)$ cross sections for most of the lighter isotopes of these elements have not been measured previously, owing to their low natural abundances.

The present results are compared with the semiempirical predictions of Pearlstein[2] and Gardner.[3] The consistent set of $(n, 2n)$ cross sections in the region $Z=40$–60 has been analyzed in terms of the statistical model, and a critical examination for possible shell effects has been made. The present results demonstrate an absence of shell-structure effects and agree better with the statistical model approach of Pearlstein[2] than with that of Gardner.[3]

---

* Work supported in part by the U.S. Atomic Energy Commission.

† Work supported by Chung Shan Institute of Science and Technology, Taiwan, Republic of China.

‡ Work supported through institutional grant from the National Aeronautics and Space Administration.

[1] D. W. Barr, C. I. Browne, and J. S. Gilmore, Phys. Rev. **123**, 859 (1961).

[2] S. Pearlstein, Nucl. Data **A3**, 327 (1967); U.S. Atomic Energy Commission Report No. BNL-897 (T-365), 1964 (unpublished).

[3] D. G. Gardner, U.S. Atomic Energy Commission Report No. UCRL-14575, 1966 (unpublished).

[4] M. Bormann, Nucl. Phys. **65**, 257 (1965).

[5] F. Manero, *International Conference on the Study of Nuclear Structure with Neutrons, Antwerp, 1965* (North-Holland Publishing Co., Amsterdam, 1966), p. 546.

[6] P. Cuzzocrea and S. Notarrigo, *International Conference on the Study of Nuclear Structure with Neutrons, Antwerp, 1965* (North-Holland Publishing Co., Amsterdam, 1966), p. 544.

[7] R. Rüder, Sitzber. Österr. Akad. Wiss. **175**, 53 (1966).

[8] J. Csikai and G. Peto, Acta Phys. Acad. Sci. Hung. **23**, 87 (1967).

[9] P. Hille, Nucl. Phys. **A107**, 49 (1968).

[10] P. Venugopala Rao and R. W. Fink, Phys. Rev. **154**, 1023 (1967).

## II. EXPERIMENTAL PROCEDURE

Neutrons were produced by the $H^3(d, n)He^4$ reaction in the Georgia Tech 200-kV accelerator. Samples usually were about 2 $cm^2$ in area and subtended an angle of ±65° to the incident deuteron beam, thus encompassing neutrons of energies 14.4±0.3 MeV. The decay of the neutron flux is monitored by a Si(Li) detector to count associated $\alpha$ particles at 90° to the beam, and the flux decay was fitted to an exponential decay curve to get the neutron flux decay constant $\Delta$. During short irradiations, the flux was kept constant. Typical neutron yields were $1\text{–}3\times10^{10}$ n/sec, and the target half-lives were around 60 min.

A coaxial 16 $cm^3$ Ge(Li) detector with resolution of about 3.6 keV full width at half-maximum (FWHM) at 1332 keV was used to measure $\gamma$ rays of energies greater than 100 keV. Low-energy $\gamma$ rays were measured with an 8-mm-diam × 5-mm-deep Ge(Li) x-ray detector, fitted with a Be window, and having resolution of about 500 eV FWHM at 14.4 keV. For each detector, a photopeak detection efficiency curve for $\gamma$ rays in the geometries used was constructed and is accurate to $\approx3\%$ based on the use of sources calibrated to 1–2%, supplied by the Int. Atomic Energy Agency, Vienna.

A fast-rabbit system (transit time $\leq1$ sec) between the neutron target and the 16-$cm^3$ Ge(Li) detector was used to measure short-lived activities, together with a digital tape recorder for rapid and successive storage of multichannel spectra (400 channels recorded on tape in 4.5 sec).

The mixed-powder method was first developed by Rao and Fink[10] and later used extensively by us[11–14] in activation cross-section measurements with thermal and 14.4-MeV neutrons. In this method, a uniform mixture is made of sample and monitor powders, where the cross section of the monitor is well known. This procedure eliminates geometrical errors present in the procedure of sandwiching foils and enables one to count sample and monitor together. In the present investigation, the reactions $Si^{28}(n, p)Al^{28}$ (2.238 min), $Al^{27}(n, p)Mg^{27}$ (9.46 min), $Fe^{56}(n, p)Mn^{56}$ (2.576 h), and $Al^{27}(n, \alpha)Na^{24}$ (14.96 h) were used as monitors, selected according to the half-life and $\gamma$-ray energy of the activity under measurement. This minimizes errors in the neutron flux decay correction and in the relative photopeak efficiency correction. Furthermore, in most of the runs mixtures containing both Fe and Al powders were used, in order to recognize from the $Mn^{56}/Na^{24}$ activity ratio any error due to nonuniform mixing of sample and monitor powders.[10] Powders of the same grain size are usually employed to make uniform mixtures. The irradiations were generally repeated at least twice.

## III. CALCULATION OF RESULTS AND ERRORS

The following equation is used to calculate the cross sections:

$$\sigma=\sigma_m\left(\frac{C\epsilon_m f_{sm} f_{am}}{C_m\epsilon f_s f_d}\right)\left(\frac{1+\alpha}{1+\alpha_m}\right)\left(\frac{N_m}{N}\right)$$

$$\times\left(\frac{\exp(-\lambda_m t_a)-\exp(-\lambda_m t_b)}{\exp(-\lambda t_a)-\exp(-\lambda t_b)}\right)\left(\frac{\lambda-\Delta}{\lambda_m-\Delta}\right)$$

$$\times\left(\frac{\exp(-\Delta T)-\exp(-\lambda_m T)}{\exp(-\Delta T)-\exp(-\lambda T)}\right), \qquad (1)$$

where subscript $m$ stands for the monitor and $\sigma$ is the cross section under study; $C$ is the total number of counts under the photopeak; $\epsilon$ is the photopeak detector efficiency; $f_s$ is the source self-absorpton correction factor; $f_d$ is the fraction of decays giving rise to the observed number of emitted $\gamma$ photons; $\alpha$ is the total internal conversion coefficient; $N$ is the number of atoms of the target isotope irradiated; $\lambda$ is the decay constant; $t_a$ is the time elapsed between the end of irradiation and the start of counting; $t_b$ is the time elapsed between end of irradiation and end of counting; $\Delta$ is the neutron flux exponential decay constant; and $T$ is the duration of the irradiation.

The following parameters were used for the monitor reactions:

$Si^{28}(n, p)Al^{28}$ (2.238 min); $E_\gamma=1780$ keV, $f_d=1.0$ (Ref. 15), $\alpha=0$, and $\sigma=252\pm15$ mb (Ref. 14); $Al^{27}(n, p)Mg^{27}$ (9.46 min), $E_\gamma=842$ keV, $f_d=0.696$ (Ref. 15), $\alpha=0$, and $\sigma=68\pm8$ mb (Ref. 14); $Fe^{56}(n, p)Mn^{56}$ (2.576 h), $E_\gamma=847$ keV, $f_d=0.9867$ (Ref. 15), $\alpha=0$, and $\sigma=100\pm6$ mb (Ref. 16); $Al^{27}(n, \alpha)Na^{24}$ (14.96 h), $E_\gamma=1369$ keV, $f_d=1.0$ (Ref. 15), $\alpha=0$, and $\sigma=114\pm6$ mb (Ref. 17).

Table I lists the results of the cross-section measurements in this work, together with the half-life of the product, the $\gamma$-ray energy, $f_d$ and $\alpha$ of the $\gamma$ rays counted.

The error limits quoted in Table I for the measured cross sections are root-mean-square errors and are composed of the following:

(i) Error in the relative photopeak efficiency of the detector. This represents the major error in the measurement, as it is not possible to get a photopeak efficiency curve to better than $\sim3\%$ accuracy, since it has to be determined with sources calibrated to an accuracy of 1–2%. In general, this error was less than 4%. Selection

---

[11] E. Kondaiah, N. RanaKumar, and R. W. Fink, Nucl. Phys. **A120**, 329 (1968).

[12] E. Kondaiah, N. RanaKumar, and R. W. Fink, Nucl. Phys. **A120**, 337 (1968).

[13] N. RanaKumar, E. Kondaiah, and R. W. Fink, Nucl. Phys. **A122**, 619 (1968).

[14] N. RanaKumar, E. Karttunen, and R. W. Fink, Nucl. Phys. **A128**, 333 (1969).

[15] C. M. Lederer *et al.*, *Table of Isotopes* (John Wiley & Sons, Inc., New York, 1967), 6th ed.

[16] H. Liskien and A. Paulsen, J. Nucl. Energy **19**, 73 (1965).

[17] H. Liskien and A. Paulsen, EURATOM Report No. EUR-119e, 1966 (unpublished).

TABLE I. Cross sections for $(n, 2n)$ reactions with 14.4±0.3-MeV neutrons from the present work.

| Reaction | Half-life | $E_\gamma$ (keV) | $f_d$ | $\alpha_{\mathrm{tot}}$[a] | Measured cross section (mb)[b] |
|---|---|---|---|---|---|
| $\mathrm{Zr}^{90}(n, 2n)\mathrm{Zr}^{89m}$ | 4.19 min | 588 | 0.94 | 0.08 | 79.5±5.6 |
| $\mathrm{Zr}^{90}(n, 2n)\mathrm{Zr}^{89g}$ | 78.4 h | 910 | 0.99 | 0.01 | 572±30 |
| $\mathrm{Zr}^{96}(n, 2n)\mathrm{Zr}^{95}$ | 65.5 day | 724<br>756 | 0.431[c]<br>0.555[c] | 0<br>0 | 1456±80 |
| $\mathrm{Nb}^{93}(n, 2n)\mathrm{Nb}^{92m}$ | 10.16 day | 934 | 0.99 | 0 | 578±30 |
| $\mathrm{Mo}^{92}(n, 2n)\mathrm{Mo}^{91m}$ | 64 sec | 658 | 0.57 | 0.055 | 16.2±1.2 |
| $\mathrm{Mo}^{92}(n, 2n)\mathrm{Mo}^{91g}$ | 15.49 min | (measured g/m = 12.4±0.6) | | | 201±17 |
| $\mathrm{Mo}^{100}(n, 2n)\mathrm{Mo}^{99}$ | 66.7 h | 740 | 0.12 | 0 | 1389±84 |
| $\mathrm{Ru}^{96}(n, 2n)\mathrm{Ru}^{95}$ | 1.65 h | 340 | 0.75 | 0 | 569±30 |
| $\mathrm{Ru}^{98}(n, 2n)\mathrm{Ru}^{97}$ | 2.88 day | 215 | 0.91 | 0 | 1169±96 |
| $\mathrm{Ru}^{104}(n, 2n)\mathrm{Ru}^{103}$ | 39.5 day | 497 | 0.88 | 0 | 1440±80 |
| $\mathrm{Rh}^{103}(n, 2n)\mathrm{Rh}^{102m}$ | 2.1 yr | 698<br>768<br>1050 | 0.422[d]<br>0.316[d]<br>0.316[d] | 0<br>0<br>0 | 435±35 |
| $\mathrm{Rh}^{103}(n, 2n)\mathrm{Rh}^{102g}$ | 206 day | 475 | 0.57 | 0 | 522±45 |
| $\mathrm{Pd}^{102}(n, 2n)\mathrm{Pd}^{101}$ | 8.4 h | 298 | 0.30 | 0 | 637±45 |
| $\mathrm{Pd}^{110}(n, 2n)\mathrm{Pd}^{109m}$ | 4.69 min | 188 | 0.58 | 0.72 | 510±35 |
| $\mathrm{Pd}^{110}(n, 2n)\mathrm{Pd}^{109g}$ | 13.5 h | 88 | 1.0 | 26.5 | 1416±150 |
| $\mathrm{Cd}^{108}(n, 2n)\mathrm{Cd}^{107}$ | 6.5 h | 93 | 1.0 | 19.7 | 865±100 |
| $\mathrm{Cd}^{110}(n, 2n)\mathrm{Cd}^{109}$ | 453 day | 88 | 1.0 | 26.5 | 1221±150 |
| $\mathrm{Cd}^{112}(n, 2n)\mathrm{Cd}^{111m}$<br>$\mathrm{Cd}^{111}(n, n')\mathrm{Cd}^{111m}$ | 48.6 min | 247 | 1.0 | 0.065 | 725±50 |
| $\mathrm{Cd}^{116}(n, 2n)\mathrm{Cd}^{115m}$ | 43 day | 934 | 0.02[e] | 0 | 569±50 |
| $\mathrm{Cd}^{116}(n, 2n)\mathrm{Cd}^{115g}$ | 2.23 day | 335 | 0.96[e] | 1.15 | 820±50 |
| $\mathrm{Sn}^{112}(n, 2n)\mathrm{Sn}^{111}(\mathrm{EC})\mathrm{In}^{111}$<br>$\mathrm{Sn}^{112}(n, np)+\cdots\mathrm{In}^{111}$ | 2.81 day | 173<br>247 | 0.99<br>0.99 | 0.115<br>0.064 | 1275±100 |
| $\mathrm{Sn}^{114}(n, 2n)\mathrm{Sn}^{113}$ | 115 day | 393 | 1.0 | 0.53 | 1239±130[f] |
| $\mathrm{Sn}^{118}(n, 2n)\mathrm{Sn}^{117m}$<br>$\mathrm{Sn}^{117}(n, n')\mathrm{Sn}^{117m}$ | 14 day | 158 | 1.0 | 0.156 | 957±100 |
| $\mathrm{Sb}^{121}(n, 2n)\mathrm{Sb}^{120m}$ | 5.8 day | 1030<br>1171 | 0.99<br>1.0 | 0<br>0 | 427±20 |
| $\mathrm{Sb}^{121}(n, 2n)\mathrm{Sb}^{120g}$ | 15.89 min | 1171 | 0.0132 | 0 | 1188±60 |
| $\mathrm{Sb}^{123}(n, 2n)\mathrm{Sb}^{122}$ | 2.8 day | 564<br>696 | 0.66<br>0.034 | 0<br>0 | 1542±80 |
| $\mathrm{Te}^{122}(n, 2n)\mathrm{Te}^{121m}$ | 154 day | 212 | 0.90 | 0.084 | 890±100 |
| $\mathrm{Te}^{122}(n, 2n)\mathrm{Te}^{121g}$ | 17 day | 573 | 0.81 | 0 | 725±40 |
| $\mathrm{Te}^{124}(n, 2n)\mathrm{Te}^{123m}$<br>$\mathrm{Te}^{123}(n, n')\mathrm{Te}^{123m}$ | 117 day | 159 | 1.0 | 0.19 | 980±100 |
| $\mathrm{Te}^{128}(n, 2n)\mathrm{Te}^{127m}$ | 109 day | 417 | 0.0082[g] | 0 | 949±150 |
| $\mathrm{Te}^{128}(n, 2n)\mathrm{Te}^{127g}$ | 9.4 h | 417 | 0.0083[g] | 0 | 712±60 |
| $\mathrm{Te}^{130}(n, 2n)\mathrm{Te}^{129m}$ | 34.1 day | 460<br>487<br>696 | 0.06[h]<br>0.0112[h]<br>0.038[h] | 0<br>0<br>0 | 885±45 |
| $\mathrm{Te}^{130}(n, 2n)\mathrm{Te}^{129g}$ | 68.7 min | 460<br>487 | 0.083[h]<br>0.0153[h] | 0<br>0 | 570±30 |

TABLE I. (*Continued.*)

| Reaction | Half-life | $E_\gamma$ (keV) | $f_d$ | $\alpha_{\text{tot}}$[a] | Measured cross section (mb) |
|---|---|---|---|---|---|
| $I^{127}(n, 2n)I^{126}$ | 12.8 day | 386 | 0.34 | 0.019 | 1649±80 |
| $Cs^{133}(n, 2n)Cs^{132}$ | 6.59 day | 668 | 0.978 | 0 | 1542±75 |
| $Ba^{130}(n, 2n)Ba^{129}(EC)Cs^{129}$ | 32.1 h | 372 | 0.36[i] | 0.05 | 1371±70 |
| $Ba^{130}(n, np)+\cdots Cs^{129}$ |  | 411 | 0.24[i] | 0.02 |  |
| $Ba^{132}(n, 2n)Ba^{131}$ | 12 day | 496 | 0.486 | 0.013 | 1574±100 |
| $Ba^{134}(n, 2n)Ba^{133m}$ | 38.9 h | 276 | 1.0 | 4.7 | 783±56 |
| $Ba^{136}(n, 2n)Ba^{135m}$ | 28.7 h | 268 | 1.0 | 5.25 | 1149±80 |
| $Ba^{135}(n, n')Ba^{135m}$ |  |  |  |  |  |
| $Ce^{136}(n, 2n)Ce^{135}$ | 17 h | 265 | 0.474[j] | 0.069 | 1318±90 |
| $Ce^{138}(n, 2n)Ce^{137m}$ | 34.4 h | 255 | 0.994 | 8.1 | 958±100 |
| $Ce^{140}(n, 2n)Ce^{139m}$ | 54 sec | 746 | 1.0 | 0.08 | 621±70 |
| $Ce^{140}(n, 2n)Ce^{139(m+g)}$ | 140 day | 165 | 1.0 | 0.24 | 1593±130 |
| $Ce^{142}(n, 2n)Ce^{141}$ | 32.5 day | 145 | 0.70 | 0.45 | 1730±170 |

[a] The conversion coefficient $\alpha_{\text{tot}}$ is taken as zero whenever it is measured or estimated to be less than 0.01.

[b] The cross sections of the reactions $Mo^{92}(n, 2n)Mo^{91m}$ and $Ce^{140}(n, 2n)Ce^{139m}$ are based on the $Si^{28}(n, p)Al^{28}$ monitor reaction with $\sigma = 252 \pm 15$ mb (Ref. 14). All other cross sections are based on the $Fe^{56}(n, p)Mn^{56}$ monitor reaction with $\sigma = 100 \pm 6$ mb (Ref. 16).

[c] L. Broman and S. Boreving, Arkiv Fysik **34,** 259 (1967).

[d] M. Adachi, H. Taketani, and K. Hisatake, J. Phys. Soc. (Japan) **24,** 227 (1968).

[e] G. Graeffe, C. W. Tang, C. D. Coryell, and G. E. Gordon, Phys. Rev **149,** 884 (1966).

[f] The measured cross section includes only 91% metastable state, but it is included as a total cross section within the error limits.

[g] *Nuclear DataSheets*, compiled by K. Way *et al.* (Printing and Publishing Office, National Academy of Sciences—National Research Council, Washington, D. C. 20418).

[h] G. Berzins, L. M. Beyer, and W. H. Kelly, Nucl. Phys. **A93,** 456 (1967).

[i] G. Graeffe and W. B. Walters, Phys. Rev. **153,** 1321 (1967).

[j] A. Abdulmalek and R. A. Nauman, Phys. Rev. **166,** 1194 (1968).

of a monitor having a $\gamma$ ray with energy close to the one under investigation helps in reducing this error.

(ii) Statistical error. This error in counting statistics was about 1%.

(iii) Error in the self-absorption correction. Thin samples were used whenever low-energy $\gamma$ rays were involved to reduce the error in this correction. In the case of low-energy $\gamma$ rays, the error in $f_s$ amounted to 1–2% at most, but is considerably lower than this for high-energy $\gamma$ rays.

(iv) Error in weighing and mixing of the samples. Weighing errors are negligible (<0.1%), but the error due to nonuniform mixing of sample and monitor powders can be comparatively high,[10] but this becomes obvious from measurement of the $Mn^{56}/Na^{24}$ activity ratio with mixed Fe and Al monitors; such spurious runs were eliminated.

(v) Errors in timing. For long irradiations and counting times, the timing errors are negligible. When short-lived activities are involved, the irradiation and counting times were measured to 0.5 sec accuracy. Spectra were taken generally with less than 20% deadtime in the analyzer, and when the deadtime changed significantly during the counting period a proper correction was made. In general, timing errors were negligible.

The errors in the monitor cross sections, and in $f_d$, $\alpha$, and half-life of the sample or monitor activities are *not* included in the reported error, because any revision in the decay schemes and conversion coefficient values permits easy recalculation of the cross sections in the future.

A discussion of cases requiring special explanation is given below.

### A. $Mo^{92}(n, 2n)Mo^{91}$ Data

As there is no $\gamma$-ray transition in $Mo^{91g}$ decay, the $m/g$ ratio was determined by following carefully the decay of the positron annihilation radiation. The $(n, 2n)$ cross section for the $Mo^{92}(n, 2n)Mo^{91m}$ (64 sec) reaction was measured by counting the 658-keV $\gamma$ ray, and the total cross section was then computed by using the $m/g$ ratio determined above.

### B. $Sn^{112}(n, 2n)Sn^{111}$ Data

Owing to the short half-life of $Sn^{111}$ (35 min), the weak $\gamma$-ray emission could not be followed because of the presence of strong interference from other activities. Therefore this cross section was determined by measuring the 2.8-day daughter activity, $In^{111}$. As the $(n, 2n)$ and the $(n, np)+\cdots$ contributions could not be separated accurately, their sum is reported in Table I.

TABLE II. Comparison of experimental $(n, 2n)$ cross sections with Pearlstein's predictions and with literature values.

| Reaction $(m+g)$ | Experimental cross section (mb) present work | Pearlstein's predicted value (mb) | Literature[a] values (mb) |
|---|---|---|---|
| $\mathrm{Zr}^{90}(n, 2n)\mathrm{Zr}^{89}$ | 652±31 | 600 | 953±97, 768±23, 502±36, 677±51, 544±22, 750±50, 800±120 |
| $\mathrm{Zr}^{96}(n, 2n)\mathrm{Zr}^{95}$ | 1456±90 | 1535 | |
| $\mathrm{Mo}^{92}(n, 2n)\mathrm{Mo}^{91}$ | 217±18 | 400 | 256±35, 158±5, 170±14, 107±7, 155±10, 132±21, 211±16, 130±29, 310±87, 315±35, 197±40 |
| $\mathrm{Mo}^{100}(n, 2n)\mathrm{Mo}^{99}$ | 1389±84 | 1560 | 1510±180, 3790±1900, 2039±210, 1910±190, 1762±200 |
| $\mathrm{Ru}^{96}(n, 2n)\mathrm{Ru}^{95}$ | 569±30 | 930 | 634±55, 478±90, 2600±300, 860±43, 616±50 |
| $\mathrm{Ru}^{98}(n, 2n)\mathrm{Ru}^{97}$ | 1168±96 | 1085 | |
| $\mathrm{Ru}^{104}(n, 2n)\mathrm{Ru}^{103}$ | 1440±80 | 1575 | 2500±500 |
| $\mathrm{Rh}^{103}(n, 2n)\mathrm{Rh}^{102}$ | 957±57 | 1405 | |
| $\mathrm{Pd}^{102}(n, 2n)\mathrm{Pd}^{101}$ | 637±45 | 1060 | |
| $\mathrm{Pd}^{110}(n, 2n)\mathrm{Pd}^{109}$ | 1416±150 | 1665 | 1948±1000, 2570±160, 2942±200, 1590±80, 1590±140 |
| $\mathrm{Cd}^{106}(n, 2n)\mathrm{Cd}^{105}$ | 975±88[b] | 975 | 827±63, 820±80, 1358±136 |
| $\mathrm{Cd}^{108}(n, 2n)\mathrm{Cd}^{107}$ | 865±100 | 1220 | 504±76 |
| $\mathrm{Cd}^{110}(n, 2n)\mathrm{Cd}^{109}$ | 1221±150 | 1410 | |
| $\mathrm{Cd}^{116}(n, 2n)\mathrm{Cd}^{115}$ | 1389±71 | 1745 | 1587±127, 1634±116, 1180±180 |
| $\mathrm{Sn}^{114}(n, 2n)\mathrm{Sn}^{113}$ | 1239±130 | 1310 | 1800±100 |
| $\mathrm{Sb}^{121}(n, 2n)\mathrm{Sb}^{120}$ | 1615±63 | 1665 | 1562±156, 1546±107, 1841±115 |
| $\mathrm{Sb}^{123}(n, 2n)\mathrm{Sb}^{122}$ | 1542±80 | 1750 | 1245±300, 1950±200, 1263±135, 1706±100, 2280±200 |
| $\mathrm{Te}^{122}(n, 2n)\mathrm{Te}^{121}$ | 1615±110 | 1500 | 1280±128 |
| $\mathrm{Te}^{128}(n, 2n)\mathrm{Te}^{127}$ | 1661±161 | 1810 | |
| $\mathrm{Te}^{130}(n, 2n)\mathrm{Te}^{129}$ | 1455±55 | 1850 | 457±120, 753±107, 676±58, 599±120 |
| $\mathrm{I}^{127}(n, 2n)\mathrm{I}^{126}$ | 1649±80 | 1720 | 1120±400, 1320±132, 1300±80, |
| $\mathrm{Xe}^{124}(n, 2n)\mathrm{Xe}^{123}$ | 1130±110[c] | 1320 | |
| $\mathrm{Xe}^{126}(n, 2n)\mathrm{Xe}^{125}$ | 1355±165[c] | 1455 | |
| $\mathrm{Xe}^{128}(n, 2n)\mathrm{Xe}^{127}$ | 1530±170[c] | 1630 | |
| $\mathrm{Xe}^{134}(n, 2n)\mathrm{Xe}^{133}$ | 1698±170[c,d] | 1800 | |
| $\mathrm{Xe}^{136}(n, 2n)\mathrm{Xe}^{135}$ | 1700±100[c] | 1930 | |
| $\mathrm{Cs}^{133}(n, 2n)\mathrm{Cs}^{132}$ | 1542±75 | 1740 | 1289±46, 1625±135, 1550±250 |

TABLE II. (*Continued.*)

| Reaction ($m+g$) | Experimental cross section (mb) present work | Pearlstein's predicted value (mb) | Literature[a] values (mb) |
|---|---|---|---|
| $Ba^{132}(n, 2n)Ba^{131}$ | 1574±100 | 1645 | |
| $Ce^{136}(n, 2n)Ce^{135}$ | 1318±90 | 1570 | |
| $Ce^{140}(n, 2n)Ce^{139}$ | 1593±130 | 1840 | 2280±200, 1804±105, 1740±100, 3000±400 |
| $Ce^{142}(n, 2n)Ce^{141}$ | 1730±170 | 1280 | 1695±102, 1600±300, 1860±170 |

[a] See CINDA–68, Index to Literature on Microscopic Neutron Data, and Supplement, U. S. Atomic Energy Commission, Division of Technical Information Extension, 1968 unpublished).

[b] Previously reported by W. Lu and R. W. Fink, Radiochim. Acta **12**, 62 (1969).

[c] From Ref. 12.

[d] Previously reported (Ref. 12) as 2360±240 mb due to an error in the photopeak efficiency.

### C. $Ba^{130}(n, 2n)Ba^{129}$ Data

The decay schemes of the $Ba^{129}$ isomers are not well known, and therefore the ($n$, $2n$) cross section was determined by observing $\gamma$ rays in the decay of 32-h $Cs^{129}$ daughter. Owing to insufficient information about the decay modes of the $Ba^{129}$ isomers, the $Ba^{130}(n, 2n)Ba^{129}(EC)Cs^{129}$ and the $Ba^{130}(n, np)+\cdots$ $Cs^{129}$ cross sections could not be separated (see Table I).

## IV. DISCUSSION

### A. Comparison of the Results with Prior Work

Most of the previous measurements were made with $\beta$-ray or $\gamma$-ray counting with NaI(Tl) detectors. $\beta$-ray counting poses the problem of resolving the continuous $\beta$ spectrum into its different half-life components and is very unreliable when many activities or thick sources are involved. $\gamma$-ray counting with NaI(Tl) detectors suffers from the defect of poor resolution. Some of the earlier results were not corrected for the decay of the neutron flux during irradiation, which can give rise to substantial errors when the activities compared do not have comparable half-lives. There are very few measurements reported with Ge(Li) detectors.

In Table II the present total ($m+g$) cross sections for the 14.4-MeV ($n$, $2n$) reactions are compared with values from the literature ($E_n$= 14–15 MeV), and with the semiempirical predictions of Pearlstein.[2] The present values, in general, agree rather well with Pearlstein's predictions, but a close examination indicates that our values are about 5–10% smaller than his predictions.

### B. ($n$, $2n$) Reaction Systematics

Taking all of the experimental values reported in the literature and plotting them against mass number in separate curves for even-$Z$ and odd-$Z$ cases, Bormann[4] observed apparent shell-structure effects around the magic neutron numbers. A similar study was made by Manero[5] and he implied that effects can also be seen at the closure of proton shells. Cuzzocrea and Notarrigo[6] reported that at neutron shell and subshell closures in the target nuclei, ($n$, $2n$) cross sections are found to increase by a factor of as much as 3. They suggested that this enhancement may be due to direct interactions. Rüder has shown that there is no significant shell effect in the ($n$, $2n$) cross sections of nuclei with neutron numbers close to 50. Csikai and Peto[8] pointed out that ($n$, $2n$) cross sections differ greatly even for different target nuclides with the *same* neutron number. No significant shell effect can be recognized when the cross sections are plotted against target neutron or mass number. They observed an $(N-Z)$ dependence of ($n$, $2n$) cross sections and suggested that it could be due to the influence of the direct inelastic scattering ($n$, $n'\gamma$) reaction. Barr *et al.*[1] noted a dependence of ($n$, $2n$) cross sections on the asymmetry parameter $(N-Z)/A$. Hille[9] pointed out that shell effects can only cause minor deviations from the smooth trend of increasing cross section with increase in $(N-Z)/A$.

By plotting our experimental values against the asymmetry parameter $(N-Z)/A$, a smoothly increasing trend appears, as shown in Fig. 1, where the error limits include possible errors in $f_d$, half-life, and $\alpha$, since they affect the trend. The error in $\sigma_m$ is not included, because as it is a systematic error, it would not affect the trend. No difference between odd-$Z$ and even-$Z$ nuclei could be discerned. It can be clearly seen that there is no shell effect corresponding to the proton-shell closure at $Z=50$. Shell effects corresponding to neutron numbers $N=50$ and 82 are also not seen. The cross sections of ${}_{54}Xe_{82}{}^{136}$ and ${}_{58}Ce_{82}{}^{140}$ also follow the general trend. The ${}_{42}Mo_{50}{}^{92}$ and ${}_{40}Zr_{50}{}^{90}$ cross sections are small and do not follow the same trend, since their thresholds are relatively high. In Fig. 2 the corresponding separation energy $S_n$ (the separation energy of the last neutron in the target nucleus), taken from Ref. 18, is plotted against $(N-Z)/A$. This also shows a similar trend, although with a bit more scattering.

---

[18] J. H. E. Mattauch, W. Thiele, and A. H. Wapstra, Nucl. Phys. **67**, 1 (1965).

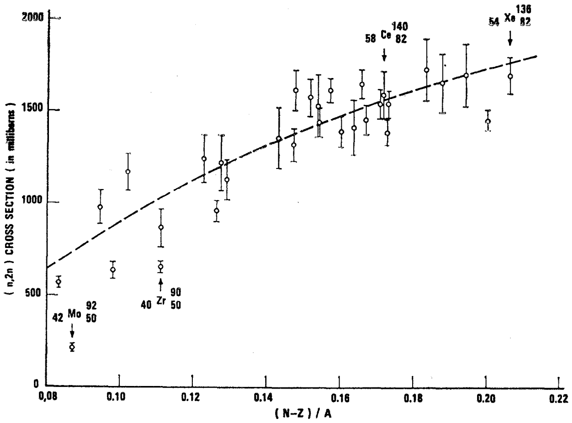

FIG. 1. Plot of experimental total (*n*, 2*n*) cross sections at 14.4 MeV from the present work against $(N-Z)/A$. The dashed curve is a least-squares fit to the empirical data. Shell-structure effects at $N=50$ and $N=82$ are not discernible.

### C. Theoretical Predictions

The theoretical (*n*, 2*n*) cross sections at a particular energy are computed from the statistical model by using the relation[2]

$$\sigma_{n,2n}=\sigma_{ne}(\sigma_{n,M}/\sigma_{ne})(\sigma_{n,2n}/\sigma_{n,M}), \tag{2}$$

where $\sigma_{ne}$ is the nonelastic cross section and $\sigma_{n,M}$ is the sum of the neutron emission cross sections $\sigma_{n,n}+\sigma_{n,2n}+\sigma_{n,3n}$, where $M=$ neutron. The variation of the nonelastic cross section with mass number is well known. Pearlstein[2] used the values given by Flerov and Talyzin's[19] empirical formula

$$\sigma_{ne}=\pi(0.12A^{1/3}+0.21)^2\,\mathrm{b}, \tag{3}$$

whereas Gardner[3] used values tabulated by Mani *et al.*[20] from optical-model potential calculations. The ratio $\sigma_{n,2n}/\sigma_{n,M}$ is calculated using the statistical model assuming that the compound nucleus emits a second neutron whenever it is energetically possible.[21] This ratio can be calculated knowing the separation energies $S_n$ and $S_{2n}$ for the first- and second-emitted neutrons and the level-density parameter $a$. It is a well established fact that the level-density parameter varies with mass number. Many authors have used such parameters as $a=A/7$, $A/10$, $A/20$, etc. Gardner[3] found that the results are not very sensitive to the change in the parameter from $A/10$ to $A/20$ and so did not use sophisticated level-density parameters incorporating shell-structure and nuclear-spin assignments. Pearlstein[2] took the effective spin values $j_Z$ and $j_N$ from Newton[22] and modified the level-density parameter to read

$$a=0.154(j_Z+j_N+1)A^{1/3}\,\mathrm{MeV}^{-1}. \tag{4}$$

By fitting experimental values of $\sigma_{n,2n}$ to curves of $\sigma_{n,2n}/\sigma_{n,M}$ generated by the model, the value of $\sigma_{n,M}$ can be determined. Knowing $\sigma_{ne}$, the ratio $\sigma_{n,M}/\sigma_{ne}$ can be calculated. Barr *et al.*[1] found an empirical fit to the ratio given by

$$\sigma_{n,M}/\sigma_{ne}=1-1.764\exp[-18.14(N-Z)/A], \tag{5}$$

which was used by Pearlstein[2] to get the ratio $\sigma_{n,M}/\sigma_{ne}$. Gardner[3] also plotted this function, but he assumed that it varies with $Z$. Pearlstein provided curves for $\sigma_{n,2n}/\sigma_{n,M}$, $\sigma_{n,M}/\sigma_{ne}$, and $\sigma_{ne}$, from which cross sections can be obtained. Gardner, on the other hand, calculated the absolute cross section for the isotope closest to the line of stability with even $N$, and used a ratio equation by which the absolute cross sections of the other isotopes of a given element are calculated by multiplying $\sigma'_{n,2n}$, calculated by the above procedure, with the ratio.

In order to test the method of Gardner, we have calculated the cross sections for Xe isotopes with both the level-density parameters $a=A/10$ and $A/20$ using his procedure. Table III lists the predictions we obtained together with the experimental values. Pearlstein's values are also given for comparison. In the Xe calculations, the isotope Xe$^{128}$ was chosen as the isotope closest to the line of stability with even $N$, and it is found that the results depend very much on which isotope is taken as the normalization point closest to stability. It can be concluded from Table III that for the Xe isotopes Gardner's ratio approach is not appropriate, as some of the predictions exceed $\sigma_{ne}$ and do not agree well with experiment, whereas the approach of Pearlstein fits better. However, Pearlstein used an empirical fit for $\sigma_{n,M}/\sigma_{ne}$ deduced from poor experimental data, as seen from Fig. 3 of Ref. 2. Therefore,

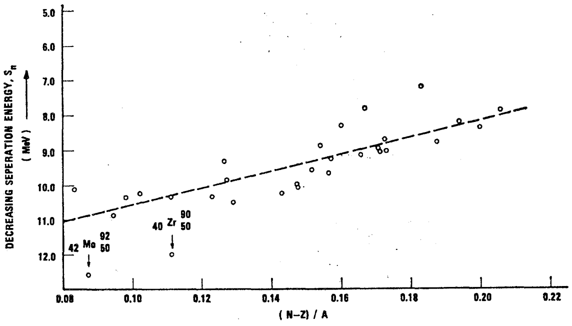

FIG. 2. Plot of neutron separation energy $S_n$ versus $(N-Z)/A$ from Ref. 18, showing the smooth dependence with $(N-Z)/A$. Error limits in some cases in $S_n$ exceed 1 MeV (e.g., for Ru$^{98}$, Cd$^{106}$, Xe$^{124}$, Xe$^{126}$, Ba$^{130}$, Ce$^{136}$). The dashed curve is a smoothed fit to the data.

---

[19] N. N. Flerov and V. M. Talyzin, J. Nucl. Energy **4**, 529 (1957).

[20] G. Mani, M. Melkanoff, and I. Iori, French Report No. CEA-2380, 1963 (unpublished).

[21] In evaluating the ratios containing $\sigma_{n,M}$, the contribution to neutron emission from the reactions (*n*, *pn*) was not included in the calculations of Pearlstein (Ref. 2) or Gardner (Ref. 3). However, in certain of the lightest isotopes of even-*Z* elements, the contribution to neutron emission from these reactions is significant or may even be the predominating one (e.g., Ni$^{58}$, Zn$^{64}$, Pd$^{102}$, Cd$^{106}$, Sn$^{112}$).

[22] T. D. Newton, Can. J. Phys. **34**, 804 (1956).

we computed a new fit for the $\sigma_{n,M}/\sigma_{ne}$ ratio by using the present experimental data, and in computing the ratio $\sigma_{n,2n}/\sigma_{n,M}$ to get $\sigma_{n,M}$, we used

$$a=0.095A^{2/3}(\bar{J}_Z+\bar{J}_N+1) \tag{6}$$

for the level-density parameter as proposed by Abdelmalek and Stavinsky.[23] With the above formula and their scheme of shell filling, very good agreement with experimental values of the level-density parameter $a$ was found. The values of $\sigma_{ne}$ used were taken from Mani *et al.*[20] and the separation energies, from Mattauch *et al.*[18] We then fitted our data to a curve represented by

$$\sigma_{n,M}/\sigma_{ne}=1-1.8124\exp[-12.99(N-Z)/A]. \tag{7}$$

The fact that the experimental values agree fairly well with the predictions (Fig. 3) based on separation energies and the level-density parameter $a$ suggests that there are no significant shell effects in the 14.4-MeV($n$, 2$n$) cross sections and that these reactions in the region of $Z=40$–60 are governed predominantly by the statistical model of the compound nucleus.

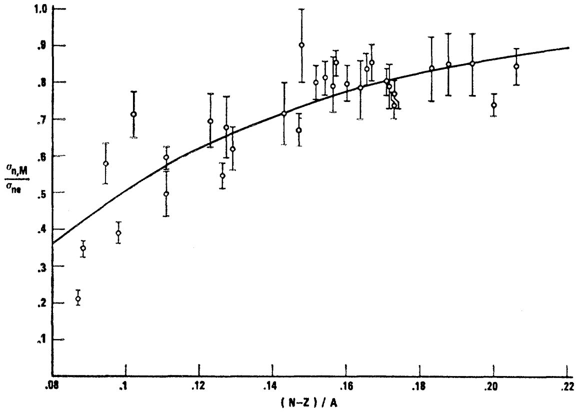

FIG. 3. Plot of $\sigma_{n,M}/\sigma_{ne}$ versus $(N-Z)/A$. The points with error limits are calculated from the present total ($n$, 2$n$) cross sections using the statistical model as described in the text. The curve is a least-squares fit to the points, to give a revision of the fitting parameters in Eq. (5) as shown by Eq. (7) in the text.

At energies above the ($n$, 3$n$) threshold, competition from the ($n$, 2$n$) reaction is assumed to be absent by Pearlstein[2] and by Gardner.[3] However, it can be seen from the results on $\mathrm{Ce}^{142}$ (for which $S_{2n}=12.65$ MeV) that the ($n$, 2$n$) reaction, in fact, predominates just above the ($n$, 3$n$) threshold. Thus, the assumption that multiple neutron emission of the highest order takes place as soon as energetically possible does not appear to be valid.

TABLE III. Comparison of 14.4-MeV predicted ($n$, 2$n$) cross sections for Xe isotopes with experimental values (in mb).

| Nuclide | Predicted according to Gardner's method[a] $a=A/10$ | $a=A/20$ | Experimental values[b] | Pearlstein's prediction[c] |
|---|---|---|---|---|
| $\mathrm{Xe}^{124}$ | 1040 | 1025 | 1130±110 | 1320 |
| $\mathrm{Xe}^{126}$ | 1320 | 1235 | 1355±165 | 1455 |
| $\mathrm{Xe}^{128}$ | 1740 | 1610 | 1530±170 | 1630 |
| $\mathrm{Xe}^{134}$ | 3525 | 2850 | 1698±170 | 1800 |
| $\mathrm{Xe}^{136}$ | 4415 | 3380 | 1700±100 | 1930 |

[a] See Ref. 3.
[b] See Ref. 12.
[c] See Ref. 2.

Gardner[3] suggested that the cross sections for all odd-$N$ target nuclides should be increased by a function $H(Z)$, which corrects for the effect of odd neutron number. This point cannot be experimentally tested by the activation method, since the products of all odd-$N$ targets are either stable or long-lived. We feel that such a correction may not be needed, as the ($n$, 2$n$) cross sections are naturally larger due to smaller neutron separation energies for odd-$N$ nuclides.

## ACKNOWLEDGMENTS

We are indebted to Richard Hobbs for operation of the 200-kV accelerator. We thank Dr. G. Gardner for helpful discussions during the course of this work.

---

[23] N. N. Abdelmalek and V. S. Stavinsky, Nucl. Phys. 58, 601 (1964).